

Supporting Information

Diameter-selective interactions between functionalized fullerenes and single-walled carbon nanotubes

Rui Zhang^{1,2}, Wanru Gao², Chang Sun², Yiwen Liu¹, Xiaojun Lu^{1,*} and Xing Lu^{2,*}

¹ Key Laboratory for Green Chemical Process of Ministry of Education, School of Chemical Engineering and Pharmacy, Wuhan Institute of Technology, Wuhan 430205, P. R. China;

² State Key Laboratory of Materials Processing and Die & Mould Technology, School of Materials Science and Engineering, Huazhong University of Science and Technology, Wuhan 430074, P. R. China;

* Correspondence: lux@hust.edu.cn (Xing Lu), xiaojunlu.sa@outlook.com (Xiaojun Lu)

Thermal gravimetric analysis for SWCNTs

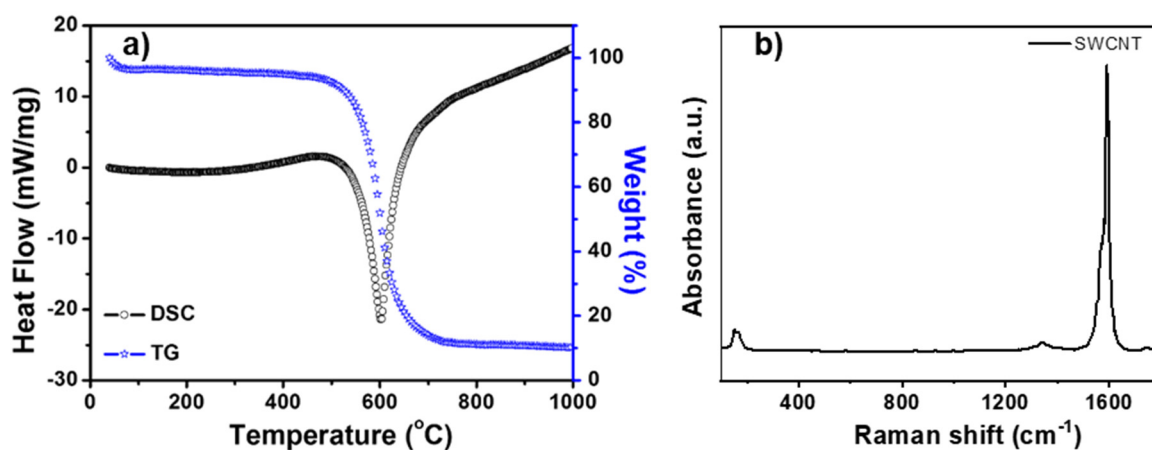


Figure S1. Thermal gravimetric analysis for SWCNTs after multi-step purification (a). The Raman spectra of SWCNT (b).

HPLC of 1

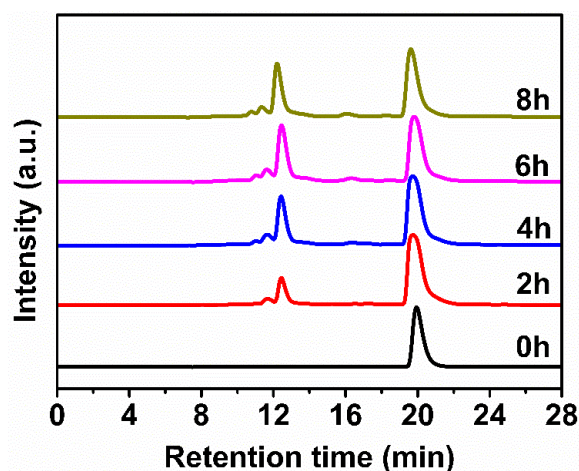


Figure S2. HPLC profiles of the reaction mixture between C₆₀ and triethylamine probed at different times at 140 °C. Conditions: Buckyprep column (Φ4.6 mm×250 mm), toluene eluent; flow rate 1.0 mL/min, detection wavelength 330 nm.

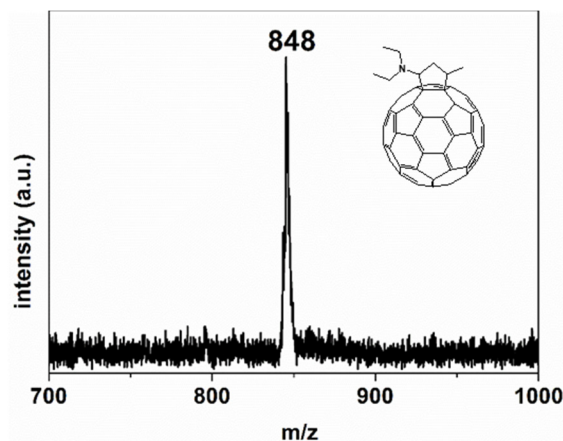


Figure S3. MALDI-TOF mass spectrum of functionalized fullerene **1**.

MALDI-TOF-MS: m/z calcd. For $C_{68}H_{18}N$ [MH] 848.14; found 848 (Figure S3).

1H NMR (600 MHz, D_4 -ODCB): δ = 4.68 (dd, J = 12.7, 4.6 Hz, 1 H), 3.58–3.43 (m, 1 H), 3.00–2.89 (m, 2 H), 2.80 (m, 2 H), 2.64 (dt, J = 12.5 Hz, 1 H), 2.51 (dt, J = 9.7, 4.6 Hz, 1 H), 1.70 (d, J = 6.8 Hz, 3 H), 1.01–0.90 (m, 6 H).

HPLC of **3**

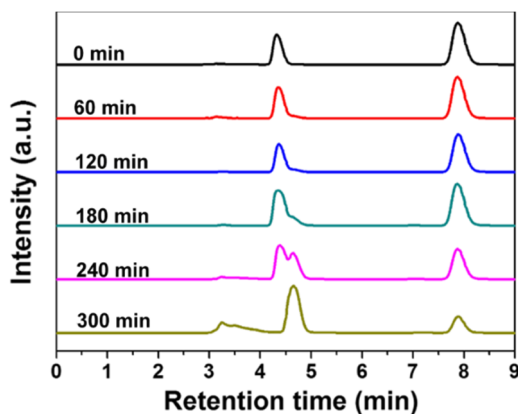


Figure S4. HPLC profiles of the reaction mixture between C_{60} and 4-(octyloxy) benzaldehyde probed at different times at 120 °C. Conditions: buckyprep column (Φ 4.6 mm \times 250 mm), toluene eluent; flow rate 1.0 mL/min, detection wavelength 290 nm.

MALDI-TOF-MS: m/z calcd. For $C_{77}H_{27}NO$ [M] 981.21; found 981.45 (Figure S3).

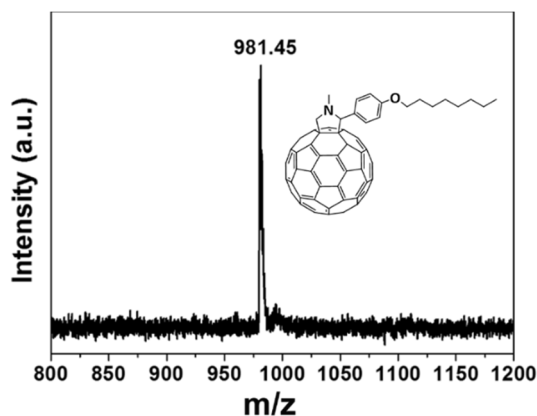


Figure S5. MALDI-TOF mass spectrum of functionalized fullerene **3**.

The MALDI-TOF mass spectrum of **3**.

^1H NMR (600 MHz, CDCl_3) δ 7.72 (s, 2H), 6.97 (d, $J = 8.1$ Hz, 2H), 5.00 (d, $J = 9.3$ Hz, 1H), 4.91 (s, 1H), 4.27 (d, $J = 9.3$ Hz, 1H), 3.98 (t, $J = 6.6$ Hz, 2H), 2.82 (s, 3H), 1.85-1.71 (m, 2H), 1.51-1.42 (m, 2H), 1.40-1.23 (m, 8H), 0.90 (t, $J = 6.8$ Hz, 3H).

^{13}C NMR (151 MHz, CDCl_3) δ 159.24, 153.71, 147.32, 146.52, 146.32, 146.28, 146.22, 146.16, 146.14, 146.11, 145.95, 145.93, 145.80, 145.55, 145.47, 145.35, 145.32, 145.28, 145.25, 145.16, 144.71, 144.63, 144.40, 143.15, 142.99, 142.68, 142.59, 142.57, 142.29, 142.26, 142.17, 142.12, 142.05, 142.02, 141.98, 141.85, 141.69, 141.54, 140.16, 140.12, 139.91, 139.59, 136.60, 135.76, 130.46, 114.59, 83.24, 77.24, 77.02, 76.81, 70.00, 68.01, 40.01, 31.82, 29.40, 29.34, 29.25, 26.09, 22.67, 14.13.

MALDI-TOF mass spectrum for C_{60}

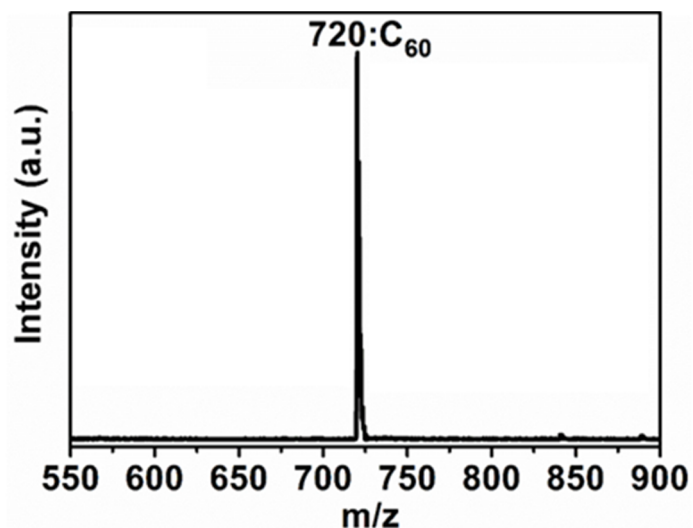


Figure S6. MALDI-TOF mass spectrum for C_{60} .

The MALDI-TOF mass spectrum of C_{60} .

Raman spectra for C_{60}

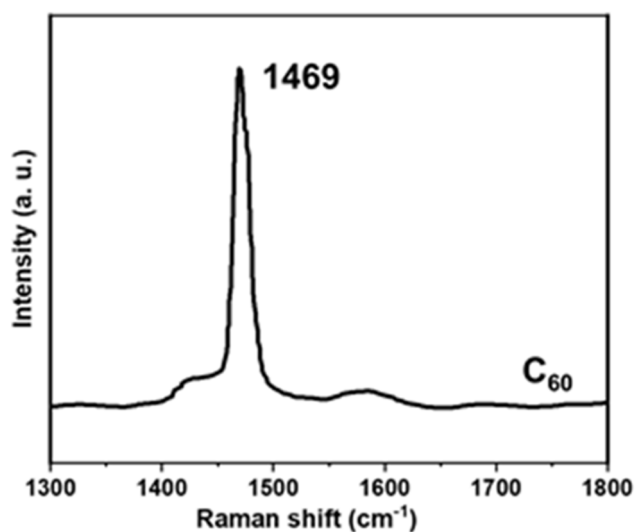


Figure S7. Raman spectra of C_{60} .

The Raman spectra of C_{60} .

The log-log UV-Vis absorption spectra of (a) C_{60} , 1, 2 and 3 dissolved in CS_2 ; (b) 1@SWCNTs, 2@SWCNTs, 3@SWCNTs, C_{60} @SWCNTs and empty SWCNTs dispersed in ethanol. Normalized UV-vis absorption spectra of (c) C_{60} , 1, 2 and 3 dissolved in CS_2 ; (d) 1@SWCNTs, 2@SWCNTs, 3@SWCNTs, C_{60} @SWCNTs and empty SWCNTs dispersed in ethanol.

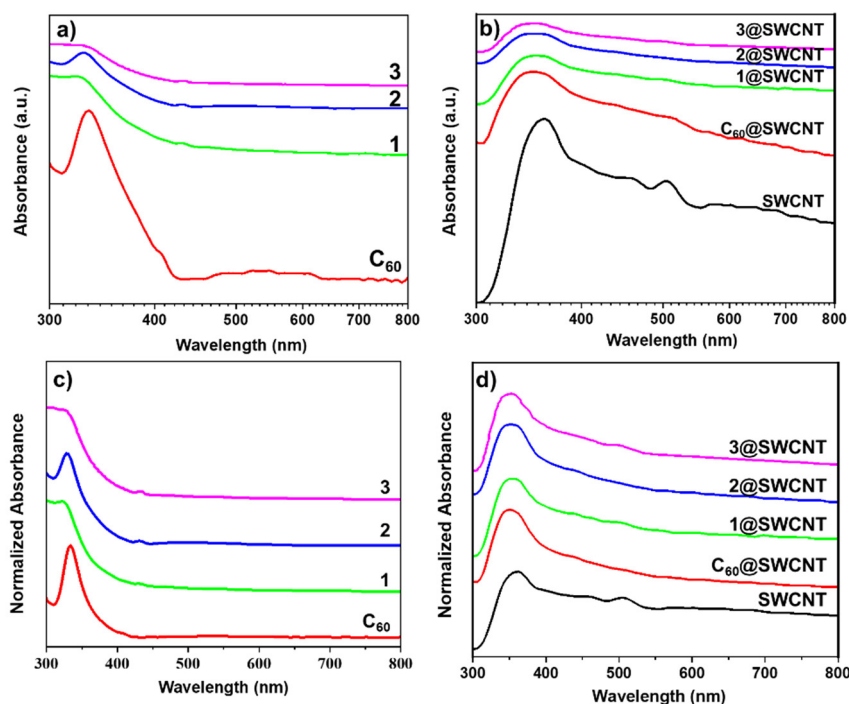


Figure S8. The log-log UV-Vis absorption spectra of (a) C_{60} , 1, 2 and 3 dissolved in CS_2 ; (b) 1@SWCNTs, 2@SWCNTs, 3@SWCNTs, C_{60} @SWCNTs and empty SWCNTs dispersed in ethanol. Normalized UV-vis absorption spectra of (c) C_{60} , 1, 2 and 3 dissolved in CS_2 ; (d) 1@SWCNTs, 2@SWCNTs, 3@SWCNTs, C_{60} @SWCNTs and empty SWCNTs dispersed in ethanol.

The log-log UV-Vis absorption spectra of C_{60} , 1, 2 and 3 are shown in Figure S8a. The log-log UV-Vis absorption spectra of 1@SWCNTs, 2@SWCNTs, 3@SWCNTs, C_{60} @SWCNTs and empty SWCNTs are shown in Figure S8b. Normalized UV-vis absorption spectra of C_{60} , 1, 2 and 3 are shown in Figure S8c. Normalized UV-vis absorption spectra of 1@SWCNTs, 2@SWCNTs, 3@SWCNTs, C_{60} @SWCNTs and empty SWCNTs are shown in Figure S8d.

Raman spectra of C_{60} @SWCNT, 1@SWCNT, 2@SWCNT and 3@SWCNT peapods and empty SWCNTs in the ranges of 1500-1700 cm^{-1}

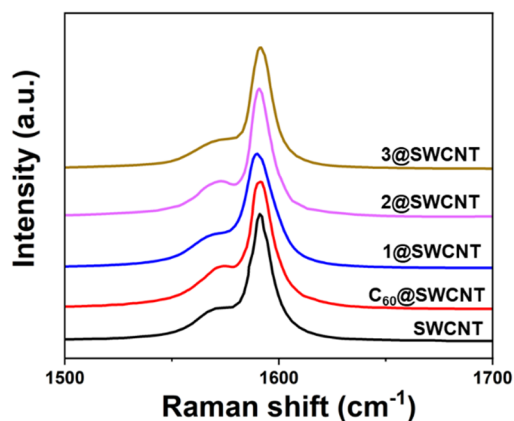


Figure S9 Raman spectra of C₆₀@SWCNT, 1@SWCNT, 2@SWCNT and 3@SWCNT peapods and empty SWCNTs in the ranges of 1500-1700 cm⁻¹.

UV-Vis absorption spectra of a) double-walled carbon nanotubes found in the literature and b) SWCNTs and peapods in this work.

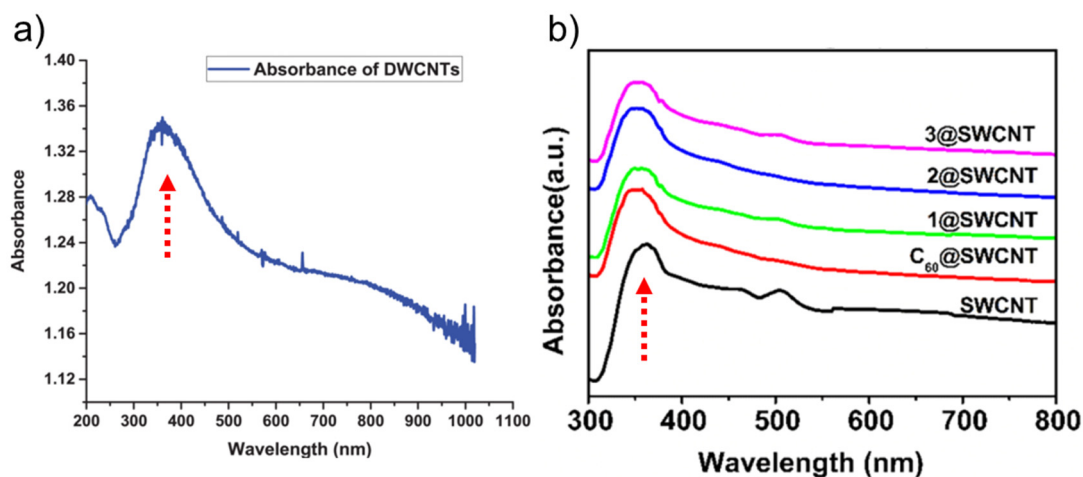


Figure S10. UV-Vis absorption spectra of a) double-walled carbon nanotubes found in [S1] and b) SWCNTs and peapods in this work. The dashed red arrows indicate the absorption band at around 300-400 nm.

According to the Rojwal's work [34] (Figure S10a), the absorption band at around 300 - 400 nm could be originated from the minor double walled CNTs in the sample.

UV-Vis absorption spectra of a) SWCNTs found in the literature and b) SWCNTs and peapods in this work.

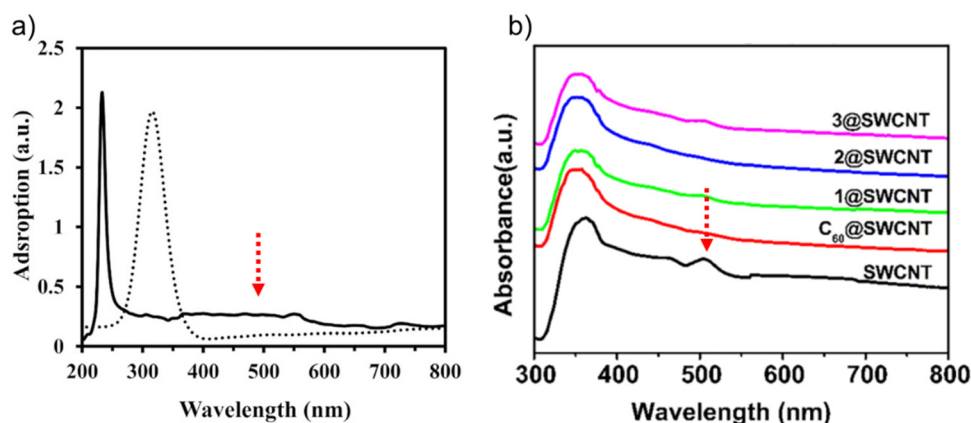


Figure S11. UV-Vis absorption spectra of a) SWCNTs found in the [S2] and b) SWCNTs and peapods in this work. The dashed red arrows indicate the absorption band at around 500 nm.

The absorption band at 500 nm could be ascribed to the SWCNT, which has also been observed Zeinabad's work [35] (Figure S11a).

UV-Vis absorption spectra of (a) 2, 2@SWCNT and SWCNT; (b) 2

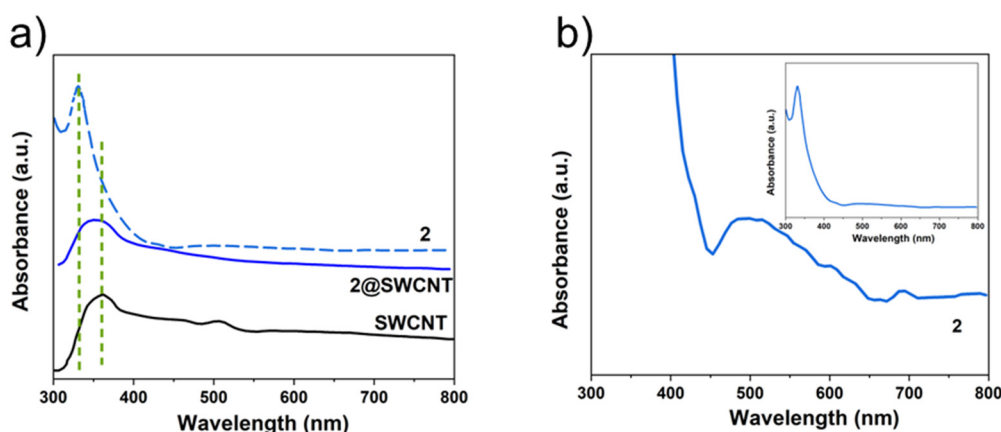


Figure S12. UV-Vis absorption spectra of (a) 2, 2@SWCNT and SWCNT; (b) 2.

As seen in Figure S12b, taking 2 as an example, the fullerene compound itself show a broad absorption in the range of 550-700 nm, which could explain the extremely broadening absorption band around 550-700 nm for the peapods.

Supplementary TEM images for estimating filling ratios

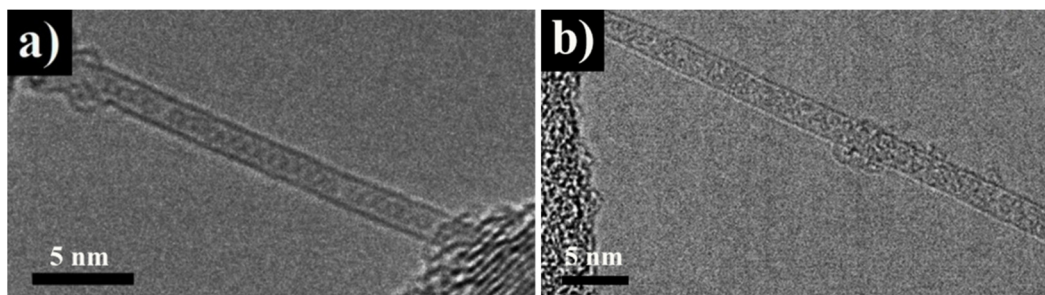


Figure S13. HR-TEM of (a) C_{60} @SWCNT peapods and (b) C_{60} @SWCNTs prepared by large-diameter SWCNTs (1.79 ~ 2.05 nm).

According to Figure S13b, the filling ratios of TEM images show over 80%.

References

34. Rojwal, V.; Singha, M.K.; Mondal, T.K. Amorphous Silicon and Carbon Nanotubes Layered Thin-Film Based Device for Temperature Sensing Application, *IEEE Sensors Journal* **2021**, *21*, 2627–2633. <https://doi.org/10.1109/JSEN.2020.3025034>.
35. Zeinabad, H.A.; Zarrabian, A.; Saboury, A.A.; Alizadeh, A.M.; Falahati, M. Interaction of Single and Multi Wall Carbon Nanotubes with the Biological Systems: Tau Protein and PC12 Cells as Targets, *Sci. Rep.* **2016**, *6*, 26508. <https://doi.org/10.1038/srep26508>.